ChemComm

A new strategy for constructing disulfide-functionalized ZIF-8 analogue using structure-directing ligand-ligand covalent interaction

Journal:	*ChemComm*
Manuscript ID	CC-COM-08-2018-007064.R1
Article Type:	Communication

Journal Name

COMMUNICATION

A new strategy for constructing disulfide-functionalized ZIF-8 analogue using structure-directing ligand-ligand covalent interaction

Received 00th January 20xx,
Accepted 00th January 20xx

DOI: 10.1039/x0xx00000x

www.rsc.org/

Yanli Gai,[a,b] Xitong Chen,[b] Huajun Yang,[c] Yanxiang Wang,[b] Xianhui Bu,*[c] and Pingyun Feng*[b]

Inter-ligand van der waals forces play a key role in ZIF framework types. Here we report an unusual case involving covalent inter-ligand interactions through disulfide bond formation in a ZIF-8 analogue. It exhibits a high CO_2 uptake, and stepwise adsorption for light hydrocarbons with potential appications in ethane/ethylene seperation.

Although metal-ligand interactions are the driving forces in the formation of coordination polymers, ligand-ligand interactions can also exhibit important impact, especially in the synthesis of zeolite imidazolate frameworks (ZIFs). ZIFs, as a subfamily of metal-organic frameworks (MOFs) with features that best mimic inorganic zeolite, have been extensively studied because of their tailorable structures and properties by custom-designed functionalization of ligand.[1] It has been well recognized that, from the synthetic perspective, ZIFs can be designed and generated by rational control of metal-ligand (M-L) interactions and ligand-ligand (L-L) van der Waals interactions where M-L interactions are the main driving forces for the ZIFs formation, while L-L noncovalent interactions between adjacent azolate ligands play a secondary role directing the final structure type.[2] Take a prototypical ZIF-8[3] as an example, if 4- and 5-positions of imidazole were substituted with benzene which provides larger steric encumbrance, it could prevent the formation of ZIF-8 type structure with SOD topology, but lead to the generation of RHO topological ZIF-11[3a] with larger cavities. Furthermore, replacing carbon atom at 5-position with nitrogen atom of benzimidazole in ZIF-11 will result in ZIF-22 with LTA topology.[2b] From the functional perspective, introduction of substituents as interaction sites with gases or reaction sites for further post-synthetically grafting functional groups could expand the pore structure, enhance and enrich functionality of ZIF-type materials. Actually, the CO_2 adsorption ability was clearly enhanced by either varying the substituent at 2-position from methyl in ZIF-8 to nitro group in ZIF-65[4] or using triazole in MAF-7[5] instead of imidazole. ZIF-90, which was also obtained by changing methyl group of ZIF-8 to aldehyde,[6] could be further functionalized through post-synthesis to remove Hg^{2+} from water or codelivery of anticancer drugs.[7]

The afore-mentioned L-L noncovalent interactions strategy to construct ZIFs with different zeotypes has been proven to be successful and fruitful. Over one hundred new ZIFs with fabulous functions have been reported within the last 10 years.[8] However, so far, the transitioning from inter-ligand noncovalent to covalent interactions in such zeotypes has rarely been seen. In this work, we propose a new strategy that involves the use of L-L covalent interactions to guide the construction of a ZIF-8 analogue, named CPM-8S herein, by judicious choice of ligand 3-thiol-1, 2, 4-triazole. In this case, it was observed that 1, 2, 4-triazole part of the ligand connects zinc using its 1- and 4-nitrogen sites to generate a sodalite network, while the 3-thiol group was oxidized and inter-connected to form disulfide bonds that tie up the sodalite cage and decorate the pore aperture. To further elucidate the structure-directing role of disulfide covalent bonds, we applied either single 1, 2, 4-triazole ligand or mixed ligands using 1, 2, 4-triazole or 2-methyl-imidazole as co-ligands to study the synthesis of targeted structures. It was found that under the same reaction condition, the 1, 2, 4-triazole results in no crystals, while the 2-methyl-imidazole has no effect on the formation of CPM-8S. These results indicate that as structure-directing agent, covalent interactions of -S-S- bonds here are more competitive than L-L van der Waals forces. Additionally, the formation of disulfide bonds not only plays a decisive structure-directing role, but also lead to a very high CO_2 uptake ability by CPM-8S. Intriguingly, CPM-8S is found to be flexible, displaying stepwise adsorption behavior toward carbon dioxide and light hydrocarbons, and this property may be useful for separating the mixture of paraffin and olefin.

[a] School of Chemistry and Materials Science, Jiangsu Normal University, Xuzhou, Jiangsu 221116, P. R. China.
[b] Department of Chemistry, University of California, Riverside, California 92521, United States. E-mail: pingyun.feng@ucr.edu
[c] Department of Chemistry and Biochemistry, California State University Long Beach, 1250 Bellflower Boulevard, Long Beach, California 90840, United States. E-mail: xianhui.bu@csulb.edu

Electronic Supplementary Information (ESI) available: Experiment detail, TG, PXRD, and additional figures of adsorption and desorption isotherms. CCDC, 1836214. See DOI: 10.1039/x0xx00000x

Highly crystalline CPM-8S, with the formula of [Zn(DS-trz)]·DMF·1/6H_2O, was prepared by solvothermal reaction of 3-thiol-1, 2, 4-triazole and zinc chloride in DMF solution. Bis(1, 2, 4-triazole-3-yl)-disulfide (abbreviated as DS-trz) was generated in situ from 3-thiol-1, 2, 4-triazole. According to the X-ray crystallographic analysis, the in situ formed disulfide in CPM-8S lowers the crystallographic symmetry from cubic, *I*43m of ZIF-8 to trigonal, *R*-3.‡ The tetrahedrally coordinated zinc ions are linked by four triazolate nitrogen atoms from three Ds-trz ligands to generate a three-dimensional zeolitic framework with a regular $4^2{\cdot}6^4$ sodalite topology (Fig. 1). The bond lengths (Zn-N) and angles (N-Zn-N) are 1.974(5), 1.978(5), 1.990(5), 1.992(6) Å and 113.52(19), 112.00(19), 105.6(2), 111.91(19), 108.87(19), 104.41(2)°, respectively.[9] The in situ formed Ds-trz displays both chelating and bridging coordination modes to link three zinc centers using its four triazolate nitrogen atoms, leaving remaining two uncoordinated triazolate nitrogen sites and disulfide groups oriented towards the hexagonal pore aperture (Fig. 1b). The bond lengths of C-S and S-S are reasonable in the range of 1.701(12)-1.772(16) Å and 1.945(11)-2.121(11) Å.[10] The sodalite cage is composed of six 4-member rings and eight elongated 6-member rings with chair configuration pulled by the disulfide. The diameter of the accessible 6-member ring aperture is measured as 4.4 Å. One DMF solvent molecule is present in the cage, and water molecule with 1/6 occupancy caused by $\bar{3}$ symmetry lies at the center of the six-member ring aperture.

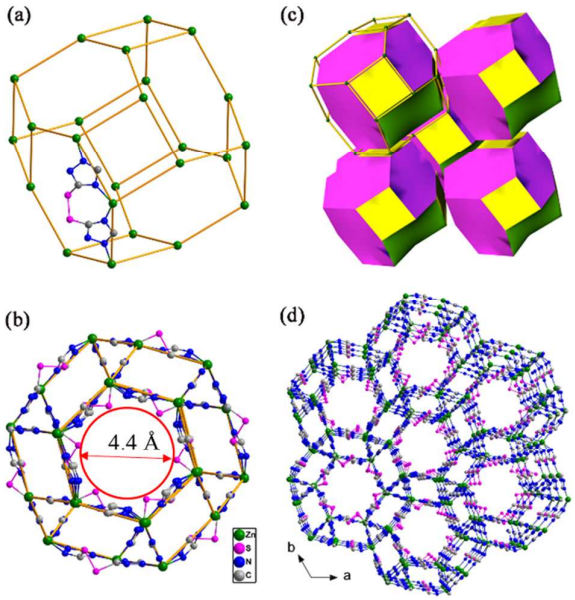

Fig. 1 (a) Sodalite cage topology of CPM-8S; (b) Sodalite cage strucutre of CPM-8S with pore aperture's diameter being 4.4 Å; (c) Tiling diagram of CPM-8S; (d) 3D structure of CPM-8S viewing along *c* axis.

Using the PLATON program, the calculated solvent-accessible volume is 53.6% of the crystal.

The purity of the as-synthesized samples was confirmed by X-ray powder diffraction (Fig. S1a). The chemical stability of CPM-8S was examined by immersing it in different solvents, such as acetone, benzene, N, N′-dimethylformamide, methanol, and water for one week at ambient temperature (Fig. S1b). Thermogravimetric analysis (Fig. S2) indicates the incorporated solvent water and DMF molecules are lost during 30-250 °C with 24.89% weight loss (the calculated value: 22.40%). No further weight loss happens until 320 °C, after which the framework starts to decompose.

The micro-porosity of CPM-8S is revealed by N_2-sorption at 77 K (Fig. S3), and the surface areas based on BET and Langmuir models are estimated to be 843 $m^2{\cdot}g^{-1}$ and 1200 $m^2{\cdot}g^{-1}$, which are lower than those of ZIF-8 (BET surface area, 1630 $m^2{\cdot}g^{-1}$; Langmuir surface area, 1810 $m^2{\cdot}g^{-1}$), due to the increased formula weight and the protrusion of disulfide groups into the cage. However, CPM-8S exhibits very high CO_2 adsorption capacity even at room temperature. Actually, the adsorption of CO_2 at 273 K (107 $cm^3{\cdot}g^{-1}$, 21.2wt%, STP) and 298 K (84 $cm^3{\cdot}g^{-1}$, 16.5wt%, STP) are much higher than those of ZIF-8 (29 $cm^3{\cdot}g^{-1}$, 273K, STP) even surpassing ZIF-69[4] (70 $cm^3{\cdot}g^{-1}$, 273K, STP) and the ZIF-8-like zeolitic MOF, IFMC[11] (91 $cm^3{\cdot}g^{-1}$, 273K, STP; 60 $cm^3{\cdot}g^{-1}$, 298K, STP) which are previously known to be among the best performing ZIF materials in CO_2 uptake. It is reasonable to suggest that in addition to the contribution of open nitrogen site that acts as Lewis base,[12] the interactions between lone-pair electrons on sulfur and electropositive carbon of CO_2 significantly attribute to the great enhancement of CO_2 capture.[13] Such consideration is further supported by the comparison to a related material MAF-7,[5] a ZIF-8-like sodalite framework constructed from 3-methyl-1, 2, 4-triazole, which was reported to exhibit CO_2 uptake of 62.5 $cm^3{\cdot}g^{-1}$ at 273 K.

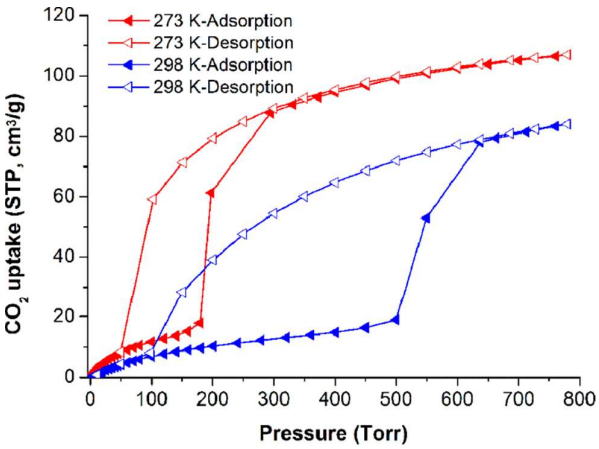

Fig. 2 CO_2 adsorption and desorption isotherms of CPM-8S at 273 K and 298K.

Interestingly, the adsorption isotherm of CO_2 displays a temperature- and pressure-dependent stepwise uptake as depicted in Fig. 2. The desorption isotherm does not retrace the adsorption isotherm, generating a pronounced hysteresis that indicates the flexible nature of CPM-8S. This behavior has rarely been observed in ZIFs especially at room temperature. Similar stepwise adsorption behaviors have, however, been observed in other flexible metal-organic frameworks for adsorption of guest molecules such as CO_2, O_2, H_2O and MeOH, wherein the flexibility-related gate-opening process caused by transformation between large-pore and small-pore phases is typically attributed to the presence of hydrogen bonding and/or electrostatic interaction between host lattices and guest molecules.[14]

Adsorption behaviors of guest-free CPM-8S toward several single-component light hydrocarbons (C_2H_6, C_2H_4, C_2H_2, and CH_4) were also measured at 298 and 273K (Fig. 3). In addition to carbon dioxide, such interesting stepwise adsorption phenomenon also occurs for C_2H_6, C_2H_4 and C_2H_2 at 273 K under certain threshold pressures as depicted in Fig. 4. It was worth noting that for ethylene, very limited amount is absorbed before 500 mmHg, after which the uptake amount abruptly increases and reaches to its saturated uptake of 88 $cm^3 \cdot g^{-1}$ (11.8wt%) at 760 mmHg. For ethane, the uptake amount increases steeply after 300 mmHg and finishes its ~90% adsorption of the saturated uptake (108 $cm^3 \cdot g^{-1}$, 13.5wt%, 760 mmHg) before 500 mmHg. The aforementioned pressure-dependent adsorption behavior creates a threshold that allows selective ethane uptake over ethylene at select pressures. It is suggested that despite the very similar size between ethane and ethylene, ethane can more readily pass through the pore aperture and penetrate into the cavity because the three-fold symmetry of methyl group is best matched and fit with the pore aperture in CPM-8S structure with $\bar{3}$ symmetry.[14a] In industry, ethane and ethylene are separated by cryogenic high-pressure distillation which is a very energy intensive process.

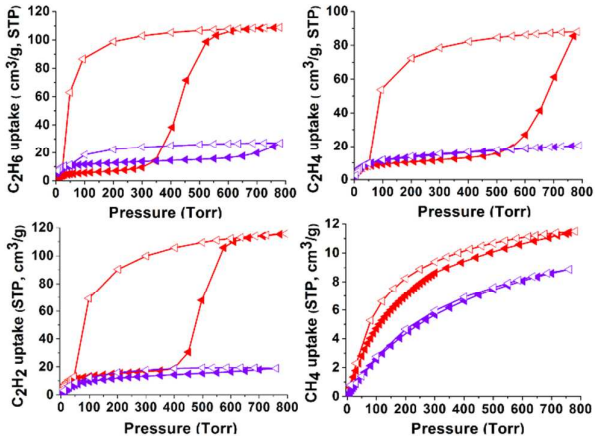

Fig. 3 Gas adsorption (solid symbol) and desorption (open symbol) isotherms for C_2H_6, C_2H_4, C_2H_2, and CH_4 at 273 K (red) and 298 K (violet).

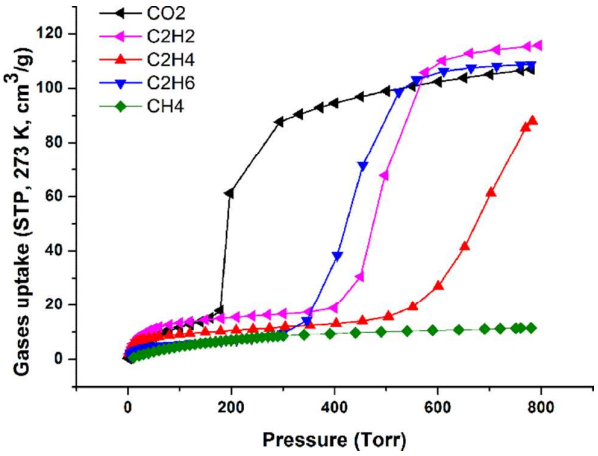

Fig. 4 Gases adsorption isotherms of carbon dioxide and light hydrocarbons of CPM-8S at 273 K with different threshold pressures.

Normally, separation of ethylene and ethane by trapping ethylene is more accessible because as a kind of unsaturated hydrocarbon, ethylene readily interacts with open metal site in porous materials,[15] while the reverse preferential adsorption of ethane over ethylene is really rare.[14a, 16] Our case may provide CPM-8S as a potential candidate in ethylene and ethane separation by ethane trapping through pressure thresholds control in a less energy demanding process.

In conclusion, a new strategy was identified here to direct the synthesis of ZIF-type material by ligand-ligand covalent interactions. Here in this study inter-ligand interactions become strongly covalent through the disulfide bond formation in a ZIF-8 analogue, CPM-8S. Specifically, two adjacent 1, 2, 4-triazolate rings are interlinked via -S-S- bonds while retaining the zeolite-type topology. Unexpectedly, instead of the increased framework rigidity from such additional linkages, CPM-8S shows a flexible framework. Such disulfide-decorated framework exhibits a very high CO_2 adsorption capacity compared with known ZIF-type materials. By virtue of the stepwise adsorption affording different pressure thresholds, such a structure is of great interest for applications in separating mixture of ethane and ethylene by trapping ethane. This design principle based on ligand-ligand covalent interactions may be extended to target new ZIFs or ZIF analogues with specific topologies or explore previous unknown ZIFs.

This work was supported by the US Department of Energy, Office of Basic Energy Sciences, Materials Sciences and Engineering Division under Award No. DE-SC0010596.

Conflicts of interest

There are no conflicts to declare.

Notes and references

‡ Crystal data for CPM-8S: trigonal, space group *R*-3, *a* = *b* = 23.390 (7) Å, *c* = 13.909(5) Åº, *V* = 6590(4) Å^3, *Z* = 18, T = 296(2) K, measured reflections 7174, independent reflections 2711, R_{int} = 0.0345, R_1 = 0.0588, wR_2 = 0.1686, *S* = 1.074.

1 (a) Y.-X. Tan, F. Wang and J. Zhang, *Chem. Soc. Rev.*, 2018, **47**, 2130; (b) S.-T. Zheng, Y. Li, T. Wu, R. A. Nieto, P. Y. Feng and X. H. Bu, *Chem. Eur. J.*, 2010, **16**, 13035. (c) T. Wu, J. Zhang, C. Zhou, L. Wang, X. Bu and P. Feng, *J. Am. Chem. Soc.,* 2009, **131**, 6111; (d) M. Eddaoudi, D. F. Sava, J. F. Eubank, K. Adil and V. Guillerm, *Chem. Soc. Rev.,* 2015, **44**, 228; (e) H.-X. Zhang, F. Wang, H. Yang, Y.-X. Tan, J. Zhang and X. Bu, *J. Am. Chem. Soc.,* 2011, **133**, 11884; (f) N. T. Nguyen, H. Furukawa, F. Gandara, H. T. Nguyen, K. E. Cordova and O. M. Yaghi, *Angew. Chem. In.t Ed.,* 2014, **53**, 10645; (g) J.-P. Zhang, Y.-B. Zhang, J.-B. Lin and X.-M. Chen, *Chem. Rev.,* 2011, **112**, 1001; (h) T. Tsoufis, C. Tampaxis, I. Spanopoulos, T. Steriotis, F. Katsaros, G. Charalambopoulou and P. N. Trikalitis, *Microporous Mesoporous Mater.,* 2018, **262**, 68.

2 (a) J. Yang, Y.-B. Zhang, Q. Liu, C. A. Trickett, E. Gutiérrez-Puebla, M. Á. Monge, H. Cong, A. Aldossary, H. Deng and O. M. Yaghi, *J. Am. Chem. Soc.,* 2017, **139**, 6448; (b) H. Hayashi, A. P. Côté, H. Furukawa, M. O'Keeffe and O. M. Yaghi, *Nat. Mater.,* 2007, **6**, 501; (c) A. Phan, C. J. Doonan, F. J. Uribe-Romo, C. B. Knobler, M. O'Keeffe and O. M. Yaghi, *Acc. Chem. Res.,* 2010, **43**, 58.

3 (a) K. S. Park, Z. Ni, A. P. Cote, J. Y. Choi, R. Huang, F. J. Uribe-Romo, H. K. Chae, M. O'Keeffe and O. M. Yaghi, *PNAS U S A,* 2006, **103**, 10186; (b) X. C. Huang, Y. Y. Lin, J. P. Zhang and X. M. Chen, *Angew Chem. Int. Ed.,* 2006, **45**, 1557.

4 R. Banerjee, A. Phan, B. Wang, C. Knobler, H. Furukawa, M. O'Keeffe and O. M. Yaghi, *Science,* 2008, **319**, 939.

5 J. P. Zhang, A. X. Zhu, R. B. Lin, X. L. Qi and X. M. Chen, *Adv. Mater,* 2011, **23**, 1268.

6 W. Morris, C. J. Doonan, H. Furukawa, R. Banerjee and O. M. Yaghi, *J. Am. Chem. Soc.,* 2008, **130**, 12626.

7 (a) S. Bhattacharjee, Y.-R. Lee and W.-S. Ahn, *CrystEngComm,* 2015, **17**, 2575; (b) F.-M. Zhang, H. Dong, X. Zhang, X.-J. Sun, M. Liu, D.-D. Yang, X. Liu and J.-Z. Wei, *ACS Appl. Mater. Interfaces,* 2017, **9**, 27332.

8 (a) C. Baerlocher and L. McCusker, Database of Zeolite Structures: http://www.iza-structure.org/databases; (b) W. Morris, N. He, K. G. Ray, P. Klonowski, H. Furukawa, I. N. Daniels, Y. A. Houndonougbo, M. Asta, O. M. Yaghi and B. B. Laird, *J. Phys. Chem. C,* 2012, **116**, 24084; (c) S.-T. Zheng, F. Zuo, T. Wu, B. Irfanoglu, C. Chou, R. A. Nieto, P. Feng and X. Bu, *Angew. Chem. Int. Ed.,* 2011, **50**, 1849; (d) Y. Q. Tian, S. Y. Yao, D. Gu, K. H. Cui, D. W. Guo, G. Zhang, Z. X. Chen and D. Y. Zhao, *Chem. Eur. J.,* 2010, **16**, 1137; (e) F. Wang, H. R. Fu, Y. Kang and J. Zhang, *Chem. Commun.,* 2014, **50**, 12065; (f) T. Wu, X. Bu, R. Liu, Z. Lin, J. Zhang and P. Feng, *Chem. Eur. J.,* 2008, **14**, 7771; (g) C. T. He, L. Jiang, Z. M. Ye, R. Krishna, Z. S. Zhong, P. Q. Liao, J. Xu, G. Ouyang, J. P. Zhang and X. M. Chen, *J. Am. Chem. Soc.,* 2015, **137**, 7217; (h) T. Wu, J. Zhang, X. Bu and P. Feng, *Chem. Mater.,* 2009, **21**, 3830; (i) K. S. Triantafyllidis, L. Nalbandian, P. N. Trikalitis, A. K. Ladavos, T. Mavromoustakos and C. P. Nicolaides, *Microporous Mesoporous Mater.,* 2004, **75**, 89.

9 (a) Z. E. Lin, Y. W. Yao, J. Zhang and G. Y. Yang, *Dalton Trans.,* 2003, **16**, 3160; (b) H.-P. Li, S.-N. Li, H.-M. Sun, M.-C. Hu, Y.-C. Jiang and Q.-G. Zhai, *Cryst. Growth Des.,* 2018, **18**, 3229.

10 (a) X.-D. Chen, H.-F. Wu and M. Du, *Chem. Commun.,* 2008, 1296; (b) S. Sanda, S. Parshamoni and S. Konar, *Inorg. Chem.,* 2013, **52**, 12866; (c) A. Azhdari Tehrani, H. Ghasempour, A. Morsali, A. Bauzá, A. Frontera and P. Retailleau, *CrystEngComm,* 2017, **19**, 1974; (d) R. Carballo, N. Fernández-Hermida, A. B. Lago, S. Rodríguez-Hermida and E. M. Vázquez-López, *Polyhedron,* 2012, **31**, 118; (e) P. Xydias, I. Spanopoulos, E. Klontzas, G. E. Froudakis and P. N. Trikalitis, *Inorg. Chem.,* 2014, **53**, 679; (f) M. C. Hong, R. Feng, F. L. Jiang, L. Chen, C. F. Yan and M. Y. Wu, *Chem. Commun.,* 2009, 5296.

11 J. S. Qin, D. Y. Du, W. L. Li, J. P. Zhang, S. L. Li, Z. M. Su, X. L. Wang, Q. Xu, K. Z. Shao and Y. Q. Lan, *Chem. Sci.,* 2012, **3**, 2114.

12 (a) H. P. Li, S. N. Li, X. Y. Hou, Y. C. Jiang, M. C. Hu and Q. G. Zhai, *Dalton Trans.,* 2018, **47**, 9310; (b) J. Park, J.-R. Li, E. Carolina Sañudo, D. Yuan and H.-C. Zhou, *Chem. Commun.,* 2012, **48**, 883; (c) W.-Y. Gao, W. Yan, R. Cai, K. Williams, A. Salas, L. Wojtas, X. Shi and S. Ma, *Chem. Commun.,* 2012, **48**, 8898; (d) J.-W. Zhang, M.-C. Hu, S.-N. Li, Y.-C. Jiang and Q.-G. Zhai, *Cryst. Growth Des.,* 2016, **16**, 6430; (e) T. Panda, P. Pachfule, Y. Chen, J. Jiang and R. Banerjee, *Chem. Commun.*, 2011, **47**, 2011.

13 (a) A. Torrisi, C. Mellot-Draznieks and R. G. Bell, *J. Chem. Phys,* 2010, **132**, 044705; (b) R. Vaidhyanathan, S. S. Iremonger, G. K. H. Shimizu, P. G. Boyd, S. Alavi and T. K. Woo, *Science,* 2010, **330**, 650; (c) N. C. Burtch, H. Jasuja, D. Dubbeldam and K. S. Walton, *J Am Chem Soc,* 2013, **135**, 7172; (d) S. Vaesen, V. Guillerm, Q. Yang, A. D. Wiersum, B. Marszalek, B. Gil, A. Vimont, M. Daturi, T. Devic, P. L. Llewellyn, C. Serre, G. Maurin and G. De Weireld, *Chem. Commun.,* 2013, **49**, 10082.

14 (a) C. Gücüyener, J. van den Bergh, J. Gascon and F. Kapteijn, *J. Am. Chem. Soc.,* 2010, **132**, 17704; (b) R. B. Lin, L. B. Li, H. Wu, H. Arman, B. Li, R. G. Lin, W. Zhou and B. L.Chen, *J. Am. Chem. Soc.,* 2017, **139**, 8022; (c) J. T. Culp, M. R. Smith, E. Bittner and B. Bockrath, *J. Am. Chem. Soc.,* 2008, **130**, 12427; (d) J. D. Pang, C. P. Liu, Y. G. Huang, M. Y. Wu, F. L. Jiang, D. Q. Yuan, F. L. Hu, K. Z. Su, G. X. Liu and M. C. Hong, *Angew. Chem. Int. Ed.,* 2016, **55**, 7478.

15 (a) J. E. Bachman, M. T. Kapelewski, D. A. Reed, M. I. Gonzalez and J. R. Long, *J. Am. Chem. Soc.,* 2017, **139**, 15363; (b) Z. R. Herm, E. D. Bloch and J. R. Long, *Chem. Mater.,* 2013, **26**, 323; (c) Y. M. Zhang, B. Y. Li, R. Krishna, Z. L. Wu, D. X. Ma, Z. Shi, T. Pham, K. Forrest, B. Space and S. Q. Ma, *Chem. Commun.,* 2015, **51**, 2714.

16 (a) P.-Q. Liao, W.-X. Zhang, J.-P. Zhang and X.-M. Chen, *Nat. commun.,* 2015, **6**, 8697; (b) J. Pires, M. L. Pinto and V. K. Saini, *ACS Appl. Mater. Interfaces,* 2014, **6**, 12093.